Model-based inference for estimating shifts in species distribution, area occupied and centre of gravity

Model-based inference for estimating shifts in species distribution, area occupied, and center of gravity

Running head: Model-based inference for distribution shifts

James T. Thorson[1*], Malin L. Pinsky[2#], Eric J. Ward[3#]

[1] Fisheries Resource Assessment and Monitoring Division (FRAM), Northwest Fisheries Science Center, National Marine Fisheries Service (NMFS), NOAA, 2725 Montlake Blvd. E, Seattle, WA 98112

[2] Department of Ecology, Evolution, and Natural Resources, Rutgers University, 14 College Farm Rd., New Brunswick, NJ 08901

[3] Conservation Biology Division, Northwest Fisheries Science Center, National Marine Fisheries Service (NMFS), NOAA, 2725 Montlake Blvd. E, Seattle, WA 98112

* Corresponding author, James.Thorson@noaa.gov

[#] MLP and EJW contributed equally

Keywords: climate change; species distribution model; range shifts; California Current; center of gravity; abundance weighted average; spatiotemporal model

Word count: 7797

Abstract

1. Changing climate is already impacting the spatial distribution of many taxa, including bees, plants, birds, butterflies, and fishes. A common goal is to detect range shifts in response to climate change, including changes in the center of the population's distribution (the center of gravity, COG), population boundaries, and area occupied. Conventional estimators, such as the abundance-weighted average (AWA) estimator for COG, confound range shifts with changes in the spatial distribution of available survey data and may be biased when the distribution of survey data shifts over time. AWA also does not estimate the standard error of COG in individual years and cannot incorporate data form multiple survey designs.
2. To explicitly account for changes in the spatial distribution of survey effort, we propose an alternative species distribution function (SDF) estimator. The SDF approach involves calculating distribution metrics, including COG, population boundary, and area occupied, directly from the predicted species distribution or density function. We illustrate the SDF approach using a spatio-temporal model that is available as an R package. Using simulated data, we confirm that the SDF substantially decreases bias in COG estimates relative to the AWA estimator. We then illustrate the method by analyzing data from two data sets spanning 1977-2013 for 18 marine fishes along the U.S. West Coast.
3. In our case study, the SDF estimator shows significant northward shifts for 6 of 18 species (with southward shifts for only 2), where two species (darkblotched and greenstriped rockfishes) have both a northward shift and a decreased area occupied. Pelagic species (e.g., Pacific hake and spiny dogfish) have more variable distribution than bottom-associated species. We also find substantial differences between AWA and SDF estimates of COG that

are likely caused by shifts in sampling distribution (which affect the AWA but not the SDF estimator).

4. We caution that common estimators for range shift can yield inappropriate inference whenever sampling designs have shifted over time. We conclude by suggesting further improvements in model-based approaches to analyzing climate impacts, including methods addressing the impact of local and regional temperature changes on species distribution.

5.

Introduction

Climate change and variability have already impacted the spatial distribution of many different taxa including butterflies (Parmesan *et al.* 1999), plants (Kelly & Goulden 2008), bees (Kerr *et al.* 2015), birds (Hitch & Leberg 2007), and marine fishes (Pinsky *et al.* 2013). Climate impacts have often been identified via changes in spatial distribution, due to the wide availability of spatially referenced survey data for many taxa as well as the relative ease of detecting changes in population distribution over time. Changes in distribution can have immediate relevance to local economies and international diplomacy (Cheung *et al.* 2012), as well as species interactions and evolutionary trajectories (Garroway *et al.* 2010). Climate change has also been documented to affect many biological processes, including the allocation of energy between growth and reproduction, community composition, and phenology (Parmesan 2006).

Estimating directional changes in a spatial distribution is not unique to population biology – similar problems exist in quantifying distributional changes in sea ice, temperature, rainfall, and patterns of disease in response to climate change. In all of these problems, it can be difficult to distinguish between long-term (multi-decadal) trends caused by anthropogenic climate change, interdecadal variability, and short-term fluctuations in spatial distribution. As a result, identifying trends in spatial distribution due to climate change generally requires analyzing data from decadal or longer time-scales (Hitch & Leberg 2007). Long time-series regarding species distribution are rare (Parmesan *et al.* 2005), and much could be learned if shorter time-series could be stitched together. However, combining data from multiple sampling protocols poses serious difficulties, including quantifying the relative performance of survey efficiency among different survey teams or sampling protocols (Sauer *et al.* 1994), accounting for spatial differences in sampling intensity, and estimating the uncertainty in any resulting estimate of

distribution. Even within a long-running survey, such as the North American Breeding Bird survey, volunteer skill and training, sampling design, and sampling effort may vary regionally and over time. For example, sampling sites may be added or removed in any given year, sampling effort may go up or down at particular sites, or the sample design itself may include random site selection (e.g., a stratified random design). Authors have tried to deal with these complications by trimming survey data to only consistently surveyed sites and time periods with consistent survey methods (Pinsky et al. 2013), or by stratifying the survey area (Rindorf & Lewy 2006; Dulvy *et al.* 2008; Engelhard *et al.* 2014). The former is often unsatisfactory because it requires discarding data. The latter estimator will eliminate the bias arising from changes in survey sampling intensity given that each stratum is sufficiently small, but will also lose precision in this case unless the average within each stratum is calculated using a shrinkage estimator (i.e., by borrowing information from nearby strata).

In this paper, we compare conventional approaches to quantifying changes in species distribution to a new model-based estimator. We first show that the conventional "abundance-weighted average" estimator for the center of a species distribution (termed the "center of gravity", COG) confounds true changes in species distribution with changes in the distribution of sampling effort. The conventional approach also does not estimate a standard error for distribution metrics, and therefore cannot distinguish between sampling variation and significant interannual variability. We then show how to estimate COG, area occupied, and population range using any model that estimates a species distribution function (SDF). SDFs are estimated by a wide class of models including, e.g., occupancy models and presence-only models. The SDF approach to estimating distribution shifts can account for shifts in sampling effort over time (or concentrations of effort in particular combinations of years and areas), separating the

observation process from the true underlying spatial distribution, and hence account for changes in survey methods or locations when combining data from multiple sampling programs. The SDF approach also estimates standard errors that can be used to distinguish whether interannual variation in distribution is biologically important or an artifact of limited sampling data. In this study, we apply the SDF estimator to data for 18 bottom-associated fishes off the U.S. West Coast, integrating data across two survey programs (1977-2004 and 2003-2013). Using the SDF model, this case-study illustrates that six species show a statistically significant, northward shift in distribution from 1977-2013, while only two show a significant southward shift. All code for replicating this analysis (as well as example data for surveys of marine fishes in the California Current, Gulf of Alaska, Eastern Bering Sea, and South Africa) is publicly available (https://github.com/nwfsc-assess/geostatistical_delta-GLMM/wiki).

Materials and Methods

A wide range of metrics have been used or proposed for understanding shifts in species distributions, including the center of gravity (COG), location of population boundaries, the area occupied, the mean temperature of occurrence, or the thermal preferences of species in a local community (Perry *et al.* 2005; Devictor *et al.* 2008). Below, we describe some of the conventional estimators as well as a novel species distribution function (SDF) approach from which a wide range of metrics can be estimated.

Conventional estimators for shifts in distribution

Conventional estimators use available data on the location of species occurrences (and often abundance as well), often processed so as to attempt to ensure comparability through time. For example, the abundance-weighted average (AWA) estimator has been widely used to track changes in the center of gravity of a population's distribution (Perry *et al.* 2005; Kelly &

121 Goulden 2008; Pinsky *et al.* 2013; Hiddink *et al.* 2015). This estimator calculates the center of
122 gravity as the average location of samples in a given year, where each location is weighted by the
123 abundance (measured either as numbers or biomass) of the species encountered at that location.
124 This estimator can be applied in multiple dimensions (e.g., latitude and longitude), but as one
125 example the latitudinal center of gravity, , is:
126 (1)
127 where n is the number of available samples, c_i is the abundance of the species in the i^{th} sample,
128 and is the latitude of the i^{th} sample. This estimator confounds changes in the spatial distribution
129 of sampling with range shifts for sampled species (see Appendix A), and therefore is only
130 suitable when the distribution of sampling is constant over time. Conventional methods for
131 calculating standard errors (e.g., sample-variance computations or nonparametric bootstrapping)
132 are not appropriate for this estimator because residuals are likely autocorrelated. The inability to
133 estimate standard errors complicates efforts to distinguish between random variation in the
134 estimator and either interannual or multiyear trends in COG. Inferring multiyear trends from the
135 AWA estimator is generally done by estimating the COG in each time period, then fitting a
136 linear regression model to estimate temporal trends. Significant trends in COG are identified
137 using a Wald test given the null hypothesis that the trend coefficient is equal to zero.
138 The same data can also be used to estimate other metrics for changes in distribution. While
139 population boundaries are difficult to observe because species detectability can decline as a
140 species become rarer, estimators for population boundaries include the absolute highest and
141 lowest latitudes at which a species is observed or an average of the three highest or lowest
142 latitudes (Perry *et al.* 2005). Similarly, area occupied can be computed as the minimum number
143 of grid cells that contain 90% of species abundance in each year (Fisher & Frank 2004). Similar

144 to the AWA estimate of COG, these metrics lack a well-defined standard error. Trends over time
145 are often detected with a linear regression model.

146 **Species distribution function (SDF) estimator for shifts in distribution**

147 As an alternative to the conventional sample-based methods, we propose a model-based
148 estimator for analyzing shifts in distribution. The model-based approach begins by defining a
149 species distribution function *d*, where the value of this function *d(s)* at any given location *s*
150 describes the expected density of the population within a spatial domain . Model parameters are
151 estimated based on available data, and parameters and data are then used to predict the species
152 distribution function at all locations within a given spatial domain. We advocate estimating
153 model parameters, predicting density , and calculating summary statistics (e.g.,) within a single
154 model, so that the standard error of the summary statistic represents estimation uncertainty for
155 model parameters. Although our case-study example includes variation over time and
156 incorporates data among different surveys, the SDF approach could also be used in simpler
157 applications (e.g., species distribution or occupancy models without any variation over time).

158 The predicted SDF can be used to calculate many possible statistics representing distribution
159 shifts, e.g., the center-of-gravity (COG), population boundaries, and area occupied by a given
160 species (Appendix B). For example, latitudinal COG can be estimated as:

161 (2)

162 where is the number of locations (e.g., grid cells) used to summarize a spatial domain, is
163 predicted density at location s_i, and is latitude for this location. This calculation (Eq. 2)
164 resembles the AWA approach (Eq. 1), except replacing a weighted average of sample locations
165 with a weighted average of predictive locations. To calculate population boundaries, we
166 calculate the cumulative distribution for abundance in northings and eastings, and then identify

167 the 5th and 95th percentiles of this cumulative distribution. For area occupied, we first estimate a
168 population kernel that summarizes the distribution of the species (Woillez *et al.* 2009), and then
169 calculate the volume of this kernel.

170 This model-based estimator provides several benefits relative to conventional estimators like
171 AWA:

172 1. It allows data from multiple sampling programs to be used when estimating shifts in
173 distribution, while controlling for changes in sampling efficiency and seasonal timing
174 between surveys;
175 2. It estimates the standard error of COG estimates, which can be used to determine whether
176 interannual variability and multiyear trends exceed the variability that is expected from
177 random chance; and
178 3. It accounts for changes in the spatial distribution of sampling effort from one year to the next
179 (whereas the AWA and other conventional estimators do not).

180 A model-based approach to estimating shifts in distribution has been used in previous ecological
181 studies (Elith *et al.* 2010; Matthews *et al.* 2011), although these have generally used habitat
182 envelope modeling (i.e., predicting density as a function of measured habitat variables) rather
183 than by estimating spatially correlated latent variables (as we do in our case study example).
184 Previous research suggests that including spatial autocorrelation will improve predictions of
185 species density compared with using only measured habitat variables (Bahn & McGill 2007;
186 Shelton *et al.* 2014), so we hypothesize that incorporating spatial autocorrelation will also
187 improve our estimates of range shifts relative to habitat envelope approaches.

188 **Applying the SDF estimator in a spatio-temporal model**

For our case-study application, we estimate the species density function $d(s,t)$ for multiple time intervals, where T is the number of modeled intervals. We use a conventional "delta-model" (also known as a "hurdle" model, (Martin *et al.* 2005)) which decomposes density $d(s,t)$ into two components: (1) the probability $p(s,t)$ of encountering the species at a given location and time; and (2) the expected density $r(s,t)$ of the species when encountered:

We specify that each of these processes follows a first-order random-walk process (Cressie & Wikle 2011), i.e., encounter probability $p(s,t)$ and expected density when encountered $r(s,t)$ in year t depend only upon their value the year before ($p(s,t-1)$ and $r(s,t-1)$) and the spatial distribution of the population is otherwise independent among years (see Appendix C for further details).

We next specify a distribution for sampling data, i.e., the probability that the i^{th} survey sample is positive (i.e., that the species is encountered) is affected by encounter probability at the location s_i and year t_i for sample i, as well as additional "catchability" variables . Similarly, the survey sample given that the species was observed follows a lognormal distribution, where the expectation is affected by expected density as well as catchability variables . Catchability variables are defined as those measurable factors that influence expected catch rates independently of changes in true density at the location of the sample. Density is calculated for a reference value of these variables, . Therefore, any process that is included as a catchability variable is "controlled for" when predicting density or associated metrics of range shift.

Parameters governing the stochastic process $p(s,t)$ and $r(s,t)$ are estimated using survey data from multiple survey designs. In the following, we assume that sampling in each year follow a probability sampling design, i.e., that there is exists some stochastic process governing the

212 spatial allocation of samples, where is the probability that location *s* will be sampled in time *t*.
213 We further assume that this sampling process is statistically independent of population density
214 *d(s,t)*. This assumption is appropriate given that the sampling follows a pre-determined protocol
215 which was designed independently from dynamics for any single species. However, the
216 assumption would be invalid in other instances, e.g., if we used data from a fishery targetting a
217 particular species. Given these two assumptions, we can estimate fixed effects by maximizing
218 the marginal likelihood of the data without explicitly estimating the sampling process during
219 parameter estimation (Cressie *et al.* 2009). In the following, we treat as fixed the coefficients for
220 measured variables, the magnitude of spatiotemporal variation, the spatial scale for encounter
221 probability and positive densities, the catchability coefficients, and the residual variance of
222 positive catch rates (see Appendix C for further details regarding parameters). We treat the
223 spatiotemporal variation as random effects, and approximate the probability of these random
224 effects using a stochastic partial differential equation approximation (Lindgren *et al.* 2011;
225 Thorson *et al.* 2015c).

226 To estimate parameters, we maximize the marginal likelihood with respect to fixed effects.
227 We approximate the marginal likelihood of fixed effects while integrating across random effects
228 via the Laplace approximation using the Template Model Builder (TMB) software (Kristensen *et*
229 *al.* In press; Kristensen 2014). Estimating the SDF model using TMB involves five steps: (1) we
230 specify the joint likelihood of data and random effects in a template file; (2) for a proposed set of
231 fixed effects, TMB identifies values of random effects that maximizes the joint likelihood; (3)
232 given these values for fixed and random effects, TMB calculates the second-derivatives of the
233 joint likelihood with respect to random effects, and calculates the Laplace approximation to the
234 marginal likelihood; (4) TMB calculates the gradient of the Laplace approximation to the

marginal likelihood with respect to fixed effects; (5) we use the marginal likelihood and its gradients via a conventional nonlinear minimizer in the R statistical environment (R Core Team 2014) to identify maximum likelihood estimates of fixed effects. Standard errors for parameters and derived quantities (e.g., the center-of-gravity) are then calculated via the inverse-Hessian matrix and delta-method.

Case study application

As a case study, we analyze two different survey data sets spanning 1977-2013 in the west coast of the USA. These surveys are designed to monitor changes in the biomass of fish populations that are targeted by commercial and recreational fisheries of the U.S. West Coast. The first survey (subsequently called the "triennial survey") was operated by the Alaska Fisheries Science Center every third year from 1977 to 2004 (for a total of 10 survey years), with an average of 484 samples per year (Weinberg *et al.* 2002). The second survey (subsequently called the "annual survey") was operated by the Northwest Fisheries Science Center every year 2003-2013 (for a total of 11 survey years), and has on average 629 samples per year (Bradburn *et al.* 2011). Triennial and annual surveys also use different vessels and sampling gear, and these differences are likely to cause differences in sampling efficiency between surveys. Pinsky et al. (2013) previously analyzed range shifts using the AWA estimator applied to data from the triennial survey, but did not incorporate data from the annual survey due to concerns about changes in survey methods. We here demonstrate the implications of analyzing data from both surveys using the conventional or SDF estimators. This demonstration serves two purposes:

1. It illustrates the potential differences in inference arising from conventional and SDF estimators when applied to data where the spatial distribution of sampling changes over time;

2. It updates the Pinsky et al. (2013) analysis when incorporating data from an additional 11 years of data (i.e., the 2003-2013 period in the annual survey).

We restrict our analysis to tows that occur within the spatial domain of both surveys, and this decreases sample sizes available for each survey (triennial: 434; annual: 412 samples per year on average). We use this restriction for both SDF and AWA estimators (although it is not necessary for the SDF estimator) to ensure that results are comparable between methods. For the AWA analysis, we fit separate linear regressions to the triennial and the annual survey data, reflecting their substantially different locations and methods.

The spatial sampling intensity function differs between the two survey designs even within the restricted area that is within the spatial domain of both surveys, and spatial sampling intensity also varies among years within a given sampling design. The two surveys also differ in seasonal timing, and likely differ in terms of sampling efficiency (a.k.a. catchability, i.e., the proportion of fish captured that are located within the sampled area). In the SDF analysis, we therefore include the following catchability variables:

1. Julian calendar date j_i for each sample; and
2. an indicator function v_i for survey (where $v_i=1$ if the sample is from the triennial survey, and zero otherwise)

such that catchability variable $z_p(i)= z_r(i)=(j_i,v_i)^{\mathrm{T}}$ for sample i. These two variables (j and v) represent linear offsets of encounter probabilities (in logit-space) and positive catch rates (in log-space). Both variables have sufficient contrast to be estimated with a low standard error, i.e., Julian calendar date has broad overlap among surveys (Fig. 1) and both annual and triennial surveys were conducted in 2004. Including these catchability covariates, while not including them when predicting density for calculating center of gravity, "filters out" the variation that is

attributable to calendar date or survey design, and species distributions and center of gravity are then predicted for a standard date (July 31st) and the triennial survey. We do not include any variables *a priori* as predictors of spatial variation in density (i.e., $x(s)$ is not included in the model), and therefore account for all spatiotemporal variation via the random-walk process ($\varepsilon_p(s,t)$ and $\varepsilon_r(s,t)$, see Appendix B). While future studies could explore oceanographic or habitat predictors of species distribution using the SDF model (Shelton *et al.* 2014), we do not do so to ensure that results are strictly comparable to the AWA estimator (which does not typically incorporate predictor variables).

For computational reasons, we approximate spatiotemporal variation ($\varepsilon(s,t)$) as being piecewise-constant at a fine spatial scale. We do this by estimating functions at $n_x=500$ "knots", which are selected via a k-means clustering algorithm applied to location of sampling data. Each location s within the survey domain then has function value $\varepsilon(s_x,t)$ where s_x is the location of the knot x that is closest to location s. We confirm that results are qualitatively similar when increasing the number of knots (i.e., $n_x=1000$). We then compare estimates of the change in distribution between AWA and SDF estimators to examine whether these two methods generate different inference regarding distribution shifts in this region.

Validation with simulated data

We also conduct a simulation experiment to illustrate the magnitude of bias that arises from using either the AWA or SDF estimators given the timing and location of samples that are available. In this experiment, we simulate population density in each of 15,979 grid cells (each is 2x2 nautical miles) that are included in the domain of the surveys in our analysis. We simulate density under four scenarios, representing (1) constant, (2) highly variable, (3) northward shifts, or (4) southward shifts in population center of gravity (Appendix E for details). We then

simulate sampling that occurs in the same years and at the same locations as in the annual and triennial surveys. We analyze the simulated data using the AWA and SDF estimators, and compare the estimate of northward COG with its true value.

Results

Changes in the distribution of sampling effort for West Coast fishes

Examination of the average latitude and longitude of survey samples in each year (Fig. 1) illustrates the magnitude of spatial changes in sampling intensity over time. In particular, the median latitude of samples was nearly 45ºN in 1986, but was close to 40ºN from 2005-2012. The distribution of the triennial survey varied greatly during the 1980s, and did not sample far south of the San Francisco Bay in 1980, 1983, and 1986 (Appendix D). Therefore, even a population that was uniformly distributed throughout this survey domain would appear to move south from the 1980s (during the early triennial sampling period) to the 2000s (during the annual sampling period).

Simulation experiment

Results from our simulation confirm that the SDF estimator greatly mitigates the bias seen in the abundance-weighted average estimator (Fig. 2). In particular, the AWA estimator is positively biased in all scenarios from 1977-2003 (i.e., during the triennial survey sampling period). This positive bias is greatest in years when the triennial survey had sampling distributed in more northerly areas (i.e., 1980, 1983, 1986). The bias is negligible for both estimators during the annual sampling period (2003-2013), and the SDF estimator has a small positive bias during early years for the "northward shift" scenario and a small negative bias for the "southward shift" scenario. Exploratory analysis indicates that the SDF estimator smooths density estimates for the unsampled, southward portion of the population domain for early years (1980, 1983, and 1986)

326 towards the estimated distribution in 1989. Decreased bias using the SDF estimator is
327 particularly evident for years 1989-2002, when the AWA is positively biased by nearly 50km,
328 while the SDF is approximately unbiased.

329 **Case study**

330 A plot of population density function *d(s,t)* for Pacific hake (Fig. 3) is characteristic of the
331 patterns estimated by the SDF model for West Coast species. For Pacific hake, the areas
332 offshore of Point Conception and the San Francisco Bay generally have high density, but density
333 near the San Francisco Bay is particularly high from 2001-2013, and areas offshore of southern
334 Oregon have particularly high densities 2003-2008. In aggregate, the population has a northward
335 distribution during 1989-2009 and relatively southward distribution in 1977-1986 and 2010-2013
336 (Fig. 4). Changes among years often exceed the standard error of the estimated center of gravity
337 (e.g., 2009 to 2010), indicating changes that are statistically significant. A comparison of the
338 model-based estimate of center of gravity and the abundance-weighted average (Fig. 4) again
339 shows large differences between estimators in 1980-1986 (when sampling had greater intensity
340 northward in the California Current) and relatively small differences 2003-2013 (when sampling
341 intensity is close to uniform north of Point Conception).

342 We next present estimates of the center-of-gravity for each of 18 species along the north-
343 south axis (i.e., to detect northward or southward movement over time, Fig. 5) for both
344 abundance-weighted average and model-based estimators (while analyzing the triennial and
345 annual surveys separately with the AWA estimator). The two estimators show different trends
346 for many species during both the triennial and annual periods, e.g., dover sole which has a
347 northward trend during the triennial period (1977-2004) in the SDF estimator but a southward
348 trend in AWA estimator. Inspecting results across species during the triennial period (1977-

2004), the AWA estimator shows a shift that is more southerly than the SDF estimator for 16 of 18 species, where this southern shift is in-line with the southern trend in the location of sampling during triennial survey (Fig. 6). In particular, the AWA estimator shows significant southward shifts for two species and northward trends for one species from 1977-2004, while the SDF estimator shows significant northward shifts for seven species and significant southward shifts for only one species. Inspecting confidence intervals in the SDF estimator (Fig. 5) also illustrates that pelagic species (Pacific hake and spiny dogfish) generally have interannual variability that is large relative to confidence interval width, whereas rockfishes generally have less evidence of interannual variability in center of gravity.

Inspecting results from the SDF estimator for each species and all available years (1977-2013) illustrates six of the species have significant northward shifts, while only two (Pacific hake and sablefish) have significant southward shifts. Both hake and sablefish have had approximately steady area-occupied during this period, so shifts in distribution have been caused by displacement of the population range, rather than expansion or contraction. Similarly, four of the six species with northward shifts have approximately steady area-occupied. However, two species (darkblotched and greenstriped rockfishes) show both significant northward shifts and substantial decreases in area occupied, indicating that the northward shift is caused by decreased density in southern habitats. This decreased density in southern habitats is also reflected in SDF estimates of the southern population boundary, which has moved northward for both species (Appendix F).

Discussion

Understanding the consequences of climate change on terrestrial and aquatic species requires unbiased estimates of how species' ranges shift. In this study, we have demonstrated that a

372 species-distribution function (SDF) estimator for distribution shifts offers three benefits over
373 conventional estimators:

374 1. The conventional metrics will provide biased estimates of distribution changes whenever
375 sampling design has changed over time. A similar bias has been previously discussed in
376 static habitat and climate envelope models, (Kadmon *et al.* 2004; Loiselle *et al.* 2008; Feeley
377 & Silman 2010), where spatial variation in sampling intensity can lead to biased estimates of
378 geographical distribution. However, spatial-varying sampling intensity has not to our
379 knowledge been discussed as causing biased estimates of changes in species distribution over
380 time. By contrast, our SDF estimator will generally be unbiased as long as changes in
381 sampling intensity are statistically independent of changes in population abundance.

382 2. The SDF estimator can incorporate information from multiple surveys simultaneously, as
383 long as there is information to inter-calibrate these surveys (e.g., samples from different
384 surveys at nearby times and locations, (Sauer *et al.* 1994)).
385 3. The SDF approach can estimate standard error estimates for each year, and therefore can be
386 used to answer whether interannual variability exceeds the level that is expected given
387 estimation error. By contrast, this task is difficult using conventional estimators, which are
388 generally interpreted by fitting a linear model to estimate a single trend over time such that
389 interannual residuals around this trend are often interpreted as statistical noise.

390 Estimated changes in species distributions can then be used to support hypotheses regarding
391 causal environmental drivers, project future change (both in habitat utilization and the ecological
392 niche that organisms inhabit), and identify management actions that may mitigate against these
393 changes.

Our case-study application involving marine species on the west coast of the USA shows that a conventional estimator can lead to inference about range shifts in the opposite direction of inference from the SDF estimator. In particular, the southerly trend in the AWA estimator for some species reflects the southward shift in sampling that occurred during the triennial survey. The SDF estimator illustrates that pelagic species (Pacific hake and spiny dogfish) exhibit substantial variability in northward center-of-gravity, and that this variability exceeds the estimated standard error for each individual year. This result supports previous observations that Pacific hake distribution varies substantially over short time periods (Agostini *et al.* 2006). Spiny dogfish has also been documented previously to have demographics that vary over time (Taylor & Gallucci 2009), but spatial variation in distribution has received less attention than for Pacific hake. By contrast, rockfishes and thornyheads (*Sebastes* and *Sebastalobus* spp.) generally have very little interannual variability in north-south distribution. These species have widely varying life history, but generally have at least some association with demersal habitats that are thought to be relatively constant through time.

We have not linked our results explicitly to environmental variables, although marine species have previously been documented to shift in distribution with temperature changes (Pinsky *et al.* 2013; Hiddink *et al.* 2015). The SDF model that we use here could be linked to climate variables in at least three alternative ways. First, an environmental variable that varies spatially (e.g., local temperature at each location s and year t) could be included as a spatial covariate in the encounter probability or positive density functions (i.e., included in $x(s,t)$) if its value is known everywhere throughout the population domain (Shelton *et al.* 2014). This approach would permit the analyst to project changes in species distribution arising from different temperature scenarios that potentially vary spatially using output downscaled climate-projection models.

417 Second, an annual time series (e.g., average regional or global temperature) could be included as
418 a covariate to predict changes in population-wide abundance, center-of-gravity, or width of the
419 population kernel. This latter approach could be used to test, e.g., whether changes in
420 temperature lead to a more concentrated population distribution. Third, temperature information
421 could be used to compute local climate velocities (i.e., the ratio of temporal and spatial gradients
422 in temperature at each location), and the spatial average of this local climate velocity could be
423 compared with population-wide changes in center of gravity to test whether the population is
424 keeping pace with local temperature shifts (Devictor *et al.* 2008; Loarie *et al.* 2009). Each
425 approach is suitable for different types of climate questions, and evaluating the relative merits of
426 each approach remains an important topic for future research.

427 We recommend further research regarding distributional changes for rare or difficult-to-
428 detect species. This can be accomplished by simultaneously estimating the distribution of rare
429 and abundant species, such that estimates for rare species "borrows information" from abundant
430 species (Ovaskainen & Soininen 2011; Thorson *et al.* 2015a). We also recommend further
431 research regarding age and size-structured species distribution models. Many species including
432 Pacific hake (Hicks *et al.* 2014), lingcod (Hamel *et al.* 2009), and summer flounder (Bell *et al.*
433 2015) are known to have different spatial distribution for old and young individuals. Given the
434 large variability in recruitment seen for most marine species (Thorson *et al.* 2014), fluctuations
435 in recruitment can therefore drive large, interannual variation in the populations center-of-
436 gravity, where years following strong recruitment are biased towards the distribution for recruits.
437 Fluctuations in distribution caused by variation in age-structure might therefore be confused with
438 climate-driven shifts in distribution, especially for short-lived species with strong cohorts (e.g.,
439 Pacific hake) or for long-lived species that rebuild their age-structure following a reduction in

fishing effort (e.g., summer flounder). Age- or size-structured distribution models could be estimated by either separately analyzing the distribution for each age or size bin, or by jointly analyzing them via some smoother across age or size (Kristensen *et al.* 2014). However, this may be complicated, given that individuals of different age or size often have different susceptibility to sampling gear. Nevertheless, we hypothesize that analyzing climatic drivers of marine species distribution may be misleading unless care is taken to control for age-based distributional effects.

Acknowledgements

We thank Aurelie Godin, Anne Boudreau, Jim Hastie, Michelle McClure, Andrew Shelton, and Jon Reum for helpful preliminary discussions, and the entire NWFSC assessment team for discussions about the shifts in sampling in the triennial survey. We also thank the many scientists and volunteers who contributed to the triennial and West Coast groundfish bottom trawl surveys. Finally, we thank Isaac Kaplan and two anonymous reviewers for helpful comments on an earlier draft.

Data accessibility

All data are publicly available from the Northwest Fisheries Science Center, National Marine Fisheries Service, NOAA. The full and up-to-date data are available at https://www.nwfsc.noaa.gov/data/, and the data set used in this analysis (which involves a restricted spatial domain and set of species) is available from Dryad, DOI:10.5061/dryad.r1s8g.

Supporting Information and Appendices

Appendix A – Statistical properties of the abundance-weighted average estimator for center of gravity

Appendix B – Detailed description of methods for the spatiotemporal species distribution function model

Appendix C – Calculating center of gravity, population boundary, the population kernel, and area occupied for the species distribution function model

Appendix D – Visualizing the spatial distribution of sampling for triennial and annual surveys

Appendix E – Details regarding a simulation experiment evaluating the likely performance of AWA and SDF estimators

Appendix F – Changes in the northern and southern population boundary for West Coast fishes

Works cited

Agostini, V.N., Francis, R.C., Hollowed, A.B., Pierce, S.D., Wilson, C. & Hendrix, A.N. (2006). The relationship between Pacific hake (Merluccius productus) distribution and poleward subsurface flow in the California Current System. *Canadian Journal of Fisheries and Aquatic Sciences*, **63**, 2648–2659.

Bahn, V. & McGill, B.J. (2007). Can niche-based distribution models outperform spatial interpolation? *Global Ecology and Biogeography*, **16**, 733–742.

Bell, R.J., Richardson, D.E., Hare, J.A., Lynch, P.D. & Fratantoni, P.S. (2015). Disentangling the effects of climate, abundance, and size on the distribution of marine fish: an example based on four stocks from the Northeast US shelf. *ICES Journal of Marine Science: Journal du Conseil*, **72**, 1311–1322.

Bradburn, M.J., Keller, A.A. & Horness, B.H. (2011). *The 2003 to 2008 US West Coast bottom trawl surveys of groundfish resources off Washington, Oregon, and California: estimates of distribution, abundance, length, and age composition*. US Department of Commerce, National Oceanic and Atmospheric Administration, National Marine Fisheries Service, Northwest Fisheries Science Center, Seattle, WA.

Cheung, W.W., Pinnegar, J., Merino, G., Jones, M.C. & Barange, M. (2012). Review of climate change impacts on marine fisheries in the UK and Ireland. *Aquatic Conservation: Marine and Freshwater Ecosystems*, **22**, 368–388.

Clark, J.S., Gelfand, A.E., Woodall, C.W. & Zhu, K. (2013). More than the sum of the parts: Forest climate response from Joint Species Distribution Models. *Ecological Applications*.

Cressie, N., Calder, C.A., Clark, J.S., Hoef, J.M.V. & Wikle, C.K. (2009). Accounting for uncertainty in ecological analysis: the strengths and limitations of hierarchical statistical modeling. *Ecological Applications*, **19**, 553–570.

Cressie, N. & Wikle, C.K. (2011). *Statistics for spatio-temporal data*. John Wiley & Sons, Hoboken, New Jersey.

Devictor, V., Julliard, R., Couvet, D. & Jiguet, F. (2008). Birds are tracking climate warming, but not fast enough. *Proceedings of the Royal Society of London B: Biological Sciences*, **275**, 2743–2748.

Dulvy, N.K., Rogers, S.I., Jennings, S., Stelzenmüller, V., Dye, S.R. & Skjoldal, H.R. (2008). Climate change and deepening of the North Sea fish assemblage: a biotic indicator of warming seas. *Journal of Applied Ecology*, **45**, 1029–1039.

Elith, J., Kearney, M. & Phillips, S. (2010). The art of modelling range-shifting species. *Methods in Ecology and Evolution*, **1**, 330–342.

Engelhard, G.H., Righton, D.A. & Pinnegar, J.K. (2014). Climate change and fishing: a century of shifting distribution in North Sea cod. *Global Change Biology*, **20**, 2473–2483.

507 Feeley, K.J. & Silman, M.R. (2010). Land-use and climate change effects on population size and
508 extinction risk of Andean plants. *Global Change Biology*, **16**, 3215–3222.

509 Fisher, J.A.D. & Frank, K.T. (2004). Abundance-distribution relationships and conservation of
510 exploited marine fishes. *Marine Ecology Progress Series*, **279**, 201–213.

511 Garroway, C.J., Bowman, J., Cascaden, T.J., Holloway, G.L., Mahan, C.G., Malcolm, J.R.,
512 Steele, M.A., Turner, G. & Wilson, P.J. (2010). Climate change induced hybridization in
513 flying squirrels. *Global Change Biology*, **16**, 113–121.

514 Hamel, O.S., Sethi, S.A. & Wadsworth, T.F. (2009). Status and future prospects for lingcod in
515 waters off Washington, Oregon, and California as assessed in 2009. *Status of the Pacific*
516 *coast groundfish fishery through*.

517 Hicks, A.C., Taylor, N., Grandin, C., Taylor, I.G. & Cox, S. (2014). *Status of the Pacific hake*
518 *(whiting) stock in U.S. and Canadian waters in 2013*.

519 Hiddink, J.G., Burrows, M.T. & García Molinos, J. (2015). Temperature tracking by North Sea
520 benthic invertebrates in response to climate change. *Global Change Biology*, **21**, 117–
521 129.

522 Hitch, A.T. & Leberg, P.L. (2007). Breeding Distributions of North American Bird Species
523 Moving North as a Result of Climate Change. *Conservation Biology*, **21**, 534–539.

524 Kadmon, R., Farber, O. & Danin, A. (2004). Effect of roadside bias on the accuracy of predictive
525 maps produced by bioclimatic models. *Ecological Applications*, **14**, 401–413.

526 Kelly, A.E. & Goulden, M.L. (2008). Rapid shifts in plant distribution with recent climate
527 change. *Proceedings of the National Academy of Sciences*, **105**, 11823–11826.

528 Kerr, J.T., Pindar, A., Galpern, P., Packer, L., Potts, S.G., Roberts, S.M., Rasmont, P.,
529 Schweiger, O., Colla, S.R., Richardson, L.L., Wagner, D.L., Gall, L.F., Sikes, D.S. &
530 Pantoja, A. (2015). Climate change impacts on bumblebees converge across continents.
531 *Science*, **349**, 177–180.

532 Kristensen, K. (2014). *TMB: General random effect model builder tool inspired by ADMB*.

533 Kristensen, K., Nielsen, A., Berg, C.W. & Skaug, H. (In press). Template Model Builder TMB.
534 *Journal of Statistical Software*.

535 Kristensen, K., Thygesen, U.H., Andersen, K.H. & Beyer, J.E. (2014). Estimating spatio-
536 temporal dynamics of size-structured populations. *Canadian Journal of Fisheries and*
537 *Aquatic Sciences*, **71**, 326–336.

538 Lindgren, F., Rue, H. & Lindström, J. (2011). An explicit link between Gaussian fields and
539 Gaussian Markov random fields: the stochastic partial differential equation approach.
540 *Journal of the Royal Statistical Society: Series B (Statistical Methodology)*, **73**, 423–498.

Loarie, S.R., Duffy, P.B., Hamilton, H., Asner, G.P., Field, C.B. & Ackerly, D.D. (2009). The velocity of climate change. *Nature*, **462**, 1052–1055.

Loiselle, B.A., Jørgensen, P.M., Consiglio, T., Jiménez, I., Blake, J.G., Lohmann, L.G. & Montiel, O.M. (2008). Predicting species distributions from herbarium collections: does climate bias in collection sampling influence model outcomes? *Journal of Biogeography*, **35**, 105–116.

Martin, T.G., Wintle, B.A., Rhodes, J.R., Kuhnert, P.M., Field, S.A., Low-Choy, S.J., Tyre, A.J. & Possingham, H.P. (2005). Zero tolerance ecology: improving ecological inference by modelling the source of zero observations. *Ecology Letters*, **8**, 1235–1246.

Matthews, S.N., Iverson, L.R., Prasad, A.M. & Peters, M.P. (2011). Changes in potential habitat of 147 North American breeding bird species in response to redistribution of trees and climate following predicted climate change. *Ecography*, **34**, 933–945.

Ovaskainen, O., Roy, D.B., Fox, R. & Anderson, B.J. (2015). Uncovering hidden spatial structure in species communities with spatially explicit joint species distribution models. *Methods in Ecology and Evolution*, n/a–n/a.

Ovaskainen, O. & Soininen, J. (2011). Making more out of sparse data: hierarchical modeling of species communities. *Ecology*, **92**, 289–295.

Parmesan, C. (2006). Ecological and evolutionary responses to recent climate change. *Annual Review of Ecology, Evolution, and Systematics*, 637–669.

Parmesan, C., Gaines, S., Gonzalez, L., Kaufman, D.M., Kingsolver, J., Townsend Peterson, A. & Sagarin, R. (2005). Empirical perspectives on species borders: from traditional biogeography to global change. *Oikos*, **108**, 58–75.

Parmesan, C., Ryrholm, N., Stefanescu, C., Hill, J.K., Thomas, C.D., Descimon, H., Huntley, B., Kaila, L., Kullberg, J., Tammaru, T. & others. (1999). Poleward shifts in geographical ranges of butterfly species associated with regional warming. *Nature*, **399**, 579–583.

Perry, A.L., Low, P.J., Ellis, J.R. & Reynolds, J.D. (2005). Climate change and distribution shifts in marine fishes. *science*, **308**, 1912–1915.

Pinsky, M.L., Worm, B., Fogarty, M.J., Sarmiento, J.L. & Levin, S.A. (2013). Marine taxa track local climate velocities. *Science*, **341**, 1239–1242.

R Core Team. (2014). *R: A Language and Environment for Statistical Computing*. R Foundation for Statistical Computing, Vienna, Austria.

Rindorf, A. & Lewy, P. (2006). Warm, windy winters drive cod north and homing of spawners keeps them there. *Journal of Applied Ecology*, **43**, 445–453.

Sauer, J.R., Peterjohn, B.G. & Link, W.A. (1994). Observer Differences in the North American Breeding Bird Survey. *The Auk*, **111**, 50–62.

Shelton, A.O., Thorson, J.T., Ward, E.J. & Feist, B.E. (2014). Spatial semiparametric models improve estimates of species abundance and distribution. *Canadian Journal of Fisheries and Aquatic Sciences*, **71**, 1655–1666.

Taylor, I.G. & Gallucci, V.F. (2009). Unconfounding the effects of climate and density dependence using 60 years of data on spiny dogfish (Squalus acanthias). *Canadian Journal of Fisheries and Aquatic Sciences*, **66**, 351–366.

Thorson, J.T., Jensen, O.P. & Zipkin, E.F. (2014). How variable is recruitment for exploited marine fishes? A hierarchical model for testing life history theory. *Canadian Journal of Fisheries and Aquatic Sciences*, **71**, 973–983.

Thorson, J.T., Scheuerell, M.D., Shelton, A.O., See, K.E., Skaug, H.J. & Kristensen, K. (2015a). Spatial factor analysis: a new tool for estimating joint species distributions and correlations in species range. *Methods in Ecology and Evolution*, **6**, 627–637.

Thorson, J.T., Shelton, A.O., Ward, E.J. & Skaug, H.J. (2015b). Geostatistical delta-generalized linear mixed models improve precision for estimated abundance indices for West Coast groundfishes. *ICES Journal of Marine Science: Journal du Conseil*, **72**, 1297–1310.

Thorson, J.T., Skaug, H.J., Kristensen, K., Shelton, A.O., Ward, E.J., Harms, J.H. & Benante, J.A. (2015c). The importance of spatial models for estimating the strength of density dependence. *Ecology*, **96**, 1202–1212.

Weinberg, K.L., Wilkins, M.E., Shaw, F.E. & Zimmermann, M. (2002). *The 2001 Pacific West Coast Bottom Trawl Survey of Groundfish Resources: Estimates of Distribution, Abundance, and Length and Age Composition*. US Department of Commerce, National Oceanic and Atmospheric Administration, National Marine Fisheries Service, Alaska Fisheries Science Center, Seattle, WA.

Woillez, M., Rivoirard, J. & Petitgas, P. (2009). Notes on survey-based spatial indicators for monitoring fish populations. *Aquatic Living Resources*, **22**, 155–164.

Zipkin, E.F., Royle, J.A., Dawson, D.K. & Bates, S. (2010). Multi-species occurrence models to evaluate the effects of conservation and management actions. *Biological Conservation*, **143**, 479–484.

606 **Figure captions**

607 Fig. 1 – Median (circle), mean (triangle), interquartile range (thick black line) and total range
608 (thin black line) for the spatial location (top row: Northings, middle row: Easting) and seasonal
609 location (bottom row: Julian calendar date starting Jan. 1) in every year of West Coast sampling
610 used in this study. The triennial survey (every third year 1977-2004) shows large differences in
611 sampling distribution relative to the annual survey (every year 2003-2013), particularly with
612 respect to Northings and Julian date

613

614 Fig. 2 – Results from the simulation experiment for four treatments involving different shifts in
615 species distribution over time (columns, see *Simulation Experiment* section of *Methods* for
616 descriptions), showing the northward center of gravity for simulated abundance (left column;
617 black line: median; shaded area: interval encompassing 80% of simulation replicates), the
618 estimated center of gravity for the species distribution function (SDF; red) and abundance-
619 weighted average (AWA; blue) estimators (middle column), and the error (Est-True) for the SDF
620 and AWA estimators (where a well-performing model will have error close to zero, as indicated
621 by the dotted line).

622

623 Fig. 3 – Estimated species distribution function $d(s,t)$ for Pacific hake in every year rescaled for
624 clarity of presentation to have a mean of one (where the colored area represents the spatial
625 domain that is included in this analysis)

626

627 Fig. 4 – Center-of-gravity for Pacific hake, shown in Universal Transverse Mercator projection
628 using Northings (top row) and Eastings (bottom row), comparing abundance-weighted average

629 (circles in left column, where light-blue indicates estimates from the triennial survey and dark-
630 blue indicates estimates from the annual survey, and the corresponding blue line is the average
631 trend from a linear regression model) and species-distribution function approaches (where the
632 thick red line is the maximum likelihood estimate and the red shaded area is +/- 1 standard error)
633
634 Fig. 5 – A comparison abundance-weighted average and species-distribution-function estimators
635 of northward distribution for all 18 West Coast species analyzed in this study (see Fig. 3 caption
636 for details)
637
638 Fig. 6 – Estimated change in northward center of gravity using data from the triennial survey
639 (1977-2004) and either the abundance-weighted-average (blue) and new species-distribution-
640 function (red) approaches, where we show a predictive distribution (centered on the maximum
641 likelihood estimates, with dispersion equal to the standard error) for each estimator, and where
642 the sign (+: positive; -: negative) and p-value (from a Wald test) are shown for each estimator
643 (red upper-left: species-distribution function; blue upper-right: abundance-weighted average),
644 and any p-value in bold font indicates a trend that is statistically significant using a two-sided
645 Wald test at 0.05 significance.
646
647 Fig. 7 – Changes over time in the area occupied by each species, calculated as the volume the
648 population kernel (an ellipse approximating the distribution that accounts for 50% of total
649 population abundance, see Appendix C) estimated from the population density function $d_p(s,t)$
650 for each species p and year t.
651

652 Fig. 8 – Estimated change in northward center of gravity using data from both triennial and
653 annual surveys (1977-2013) and the new species-distribution-function (red) approaches, where
654 we show a predictive distribution (centered on the maximum likelihood estimates, with
655 dispersion equal to the standard error), where the sign (+: positive; -: negative) and p-value (from
656 a Wald test) is shown in the upper-left, and any p-value in bold font indicates a trend that is
657 statistically significant using a two-sided Wald test at 0.05 significance.
658

659 **Fig. 1**

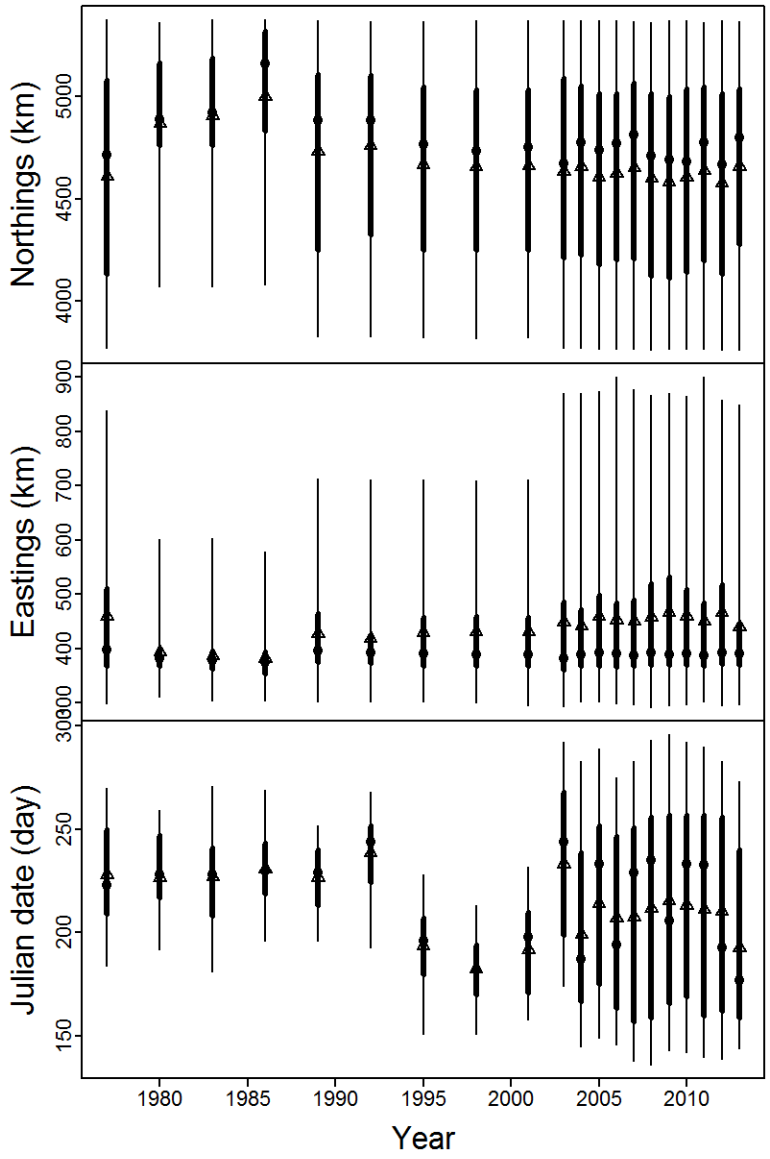

660

661

662 **Fig. 2**

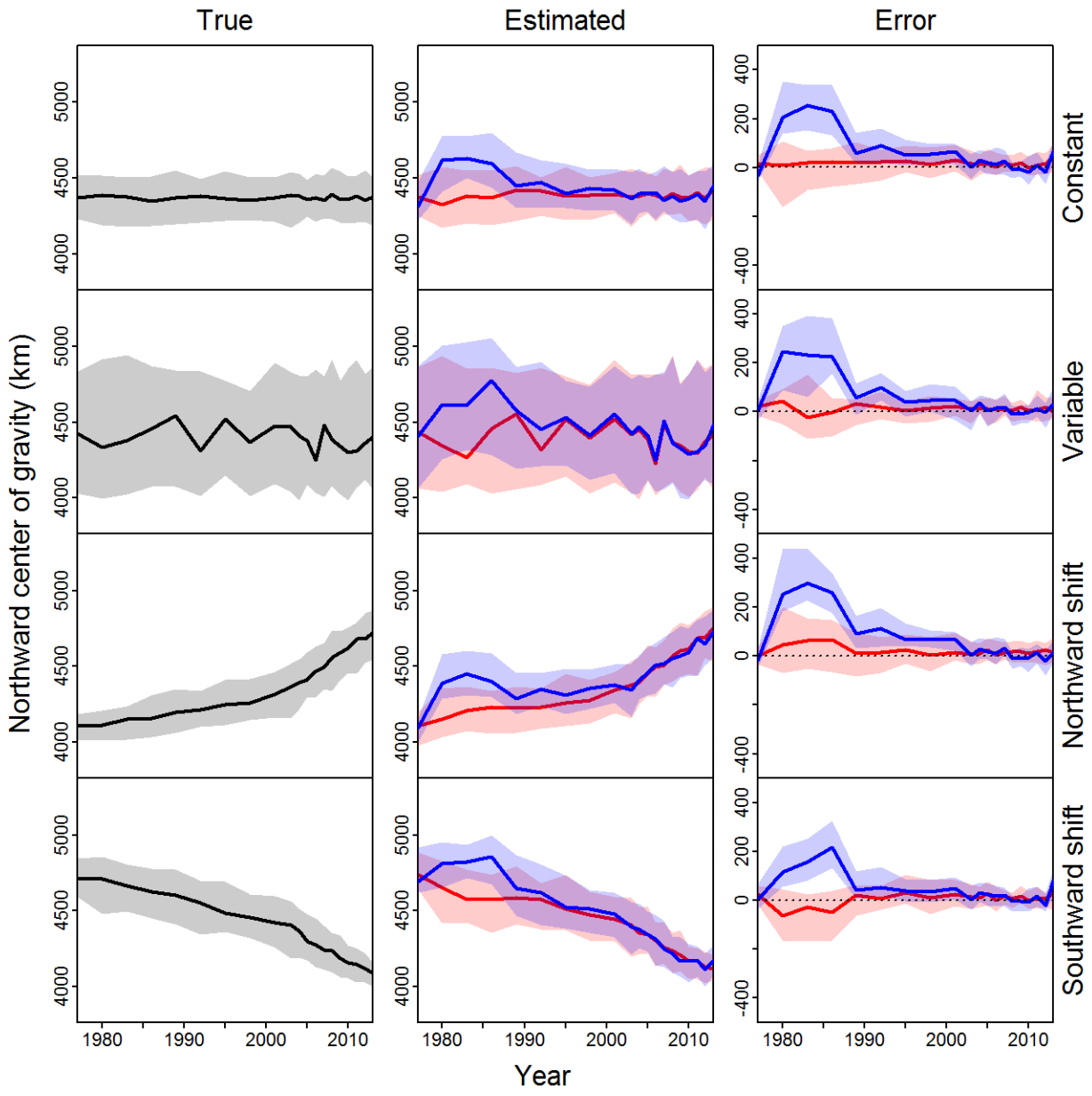

663

664

665 **Fig. 3**

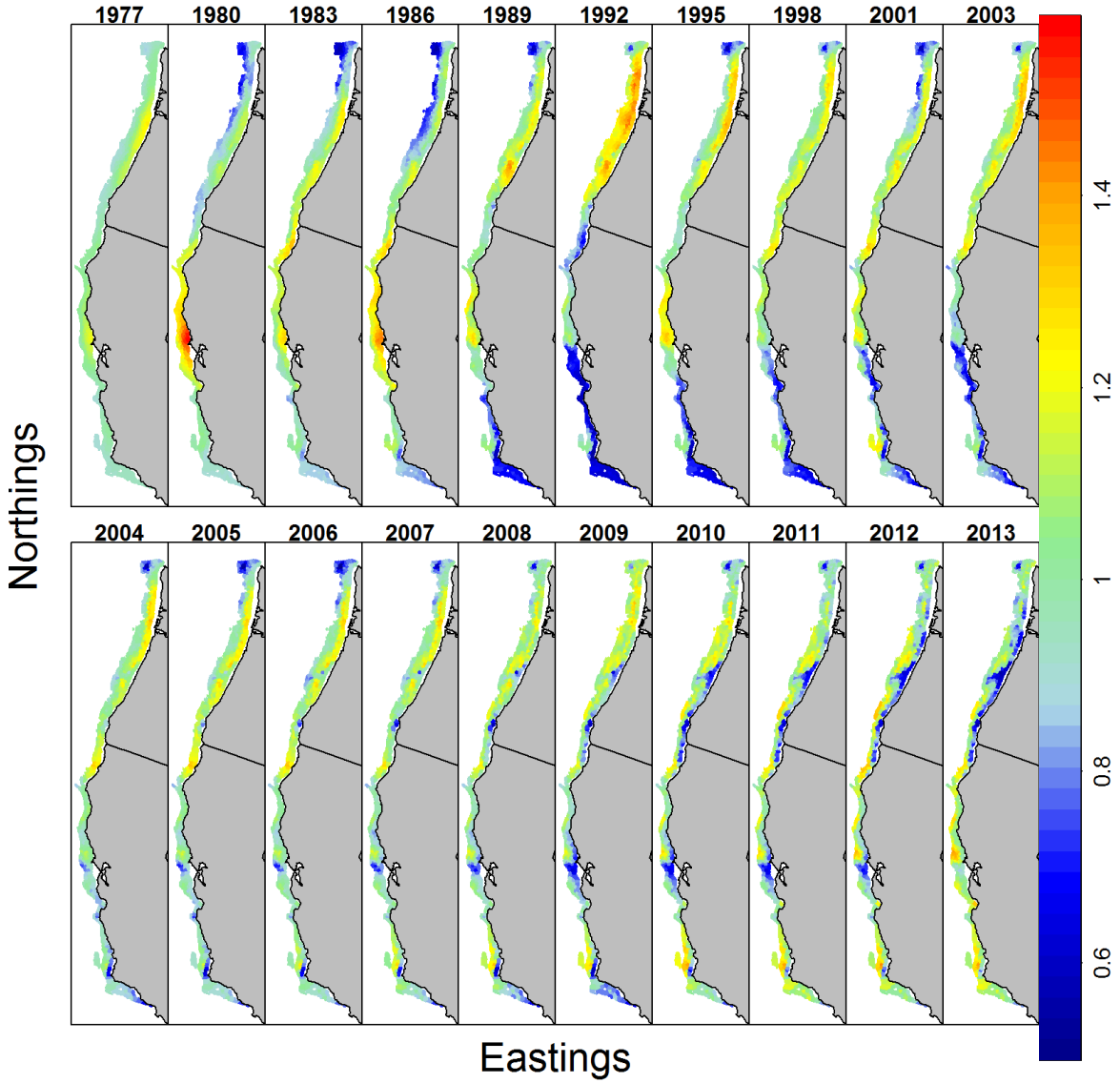
1977
1980
1983
1986
1989
1992
1995
1998
2001
2003
2004
2005
2006
2007
2008
2009
2010
2011
2012
2013
Northings
Eastings
1.4
1.2
1
0.8
0.6

666

667 **Fig. 4**

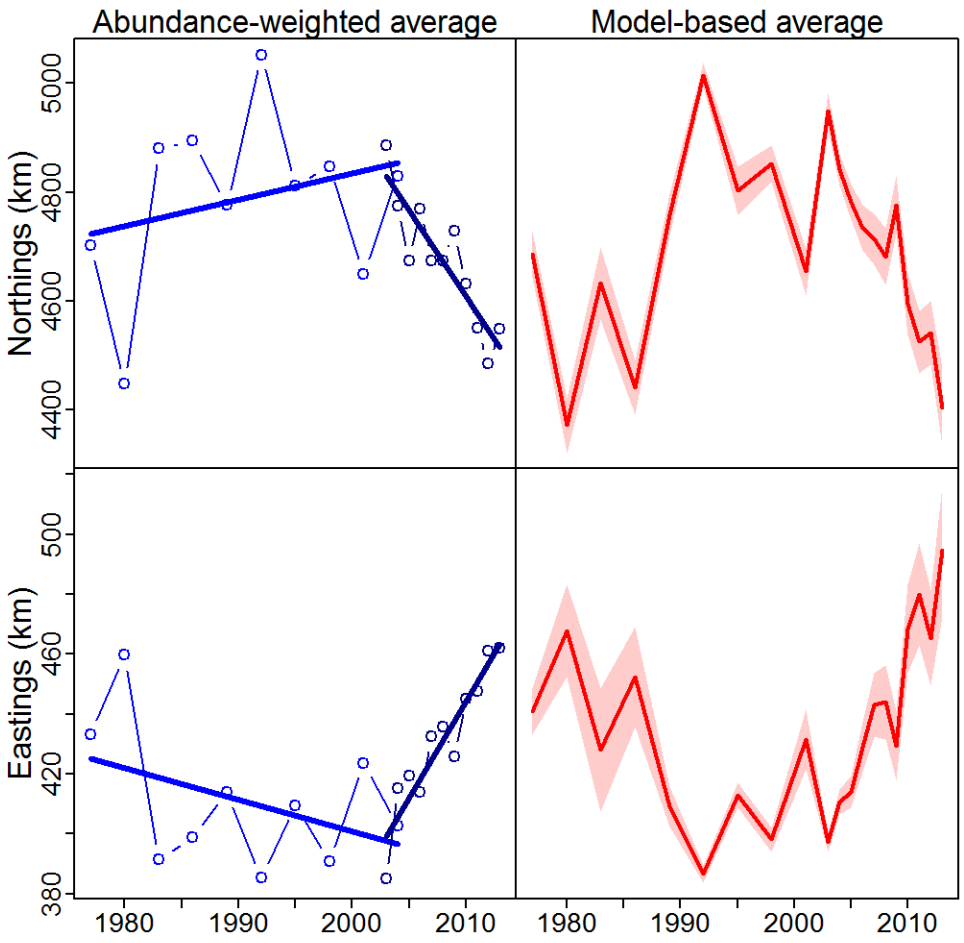
Abundance-weighted average
Model-based average
Northings (km)
4400
4600
4800
5000
Eastings (km)
380
420
460
500
1980
1990
2000
2010

668

669 **Fig. 5**

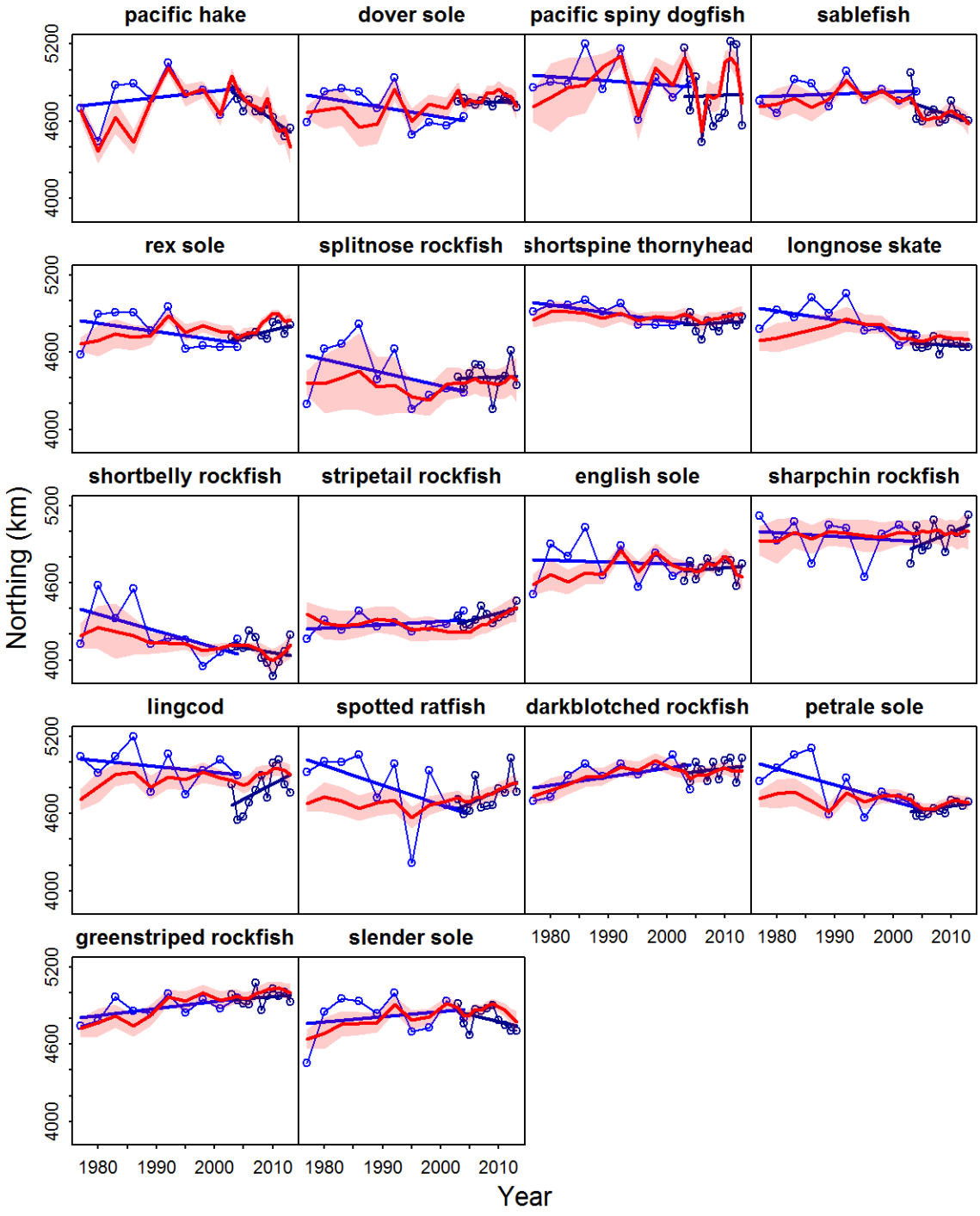
pacific hake
dover sole
pacific spiny dogfish
sablefish
rex sole
splitnose rockfish
shortspine thornyhead
longnose skate
shortbelly rockfish
stripetail rockfish
english sole
sharpchin rockfish
lingcod
spotted ratfish
darkblotched rockfish
petrale sole
greenstriped rockfish
slender sole
Northing (km)
4000
4600
5200
1980
1990
2000
2010
Year

670

671 **Fig. 6**

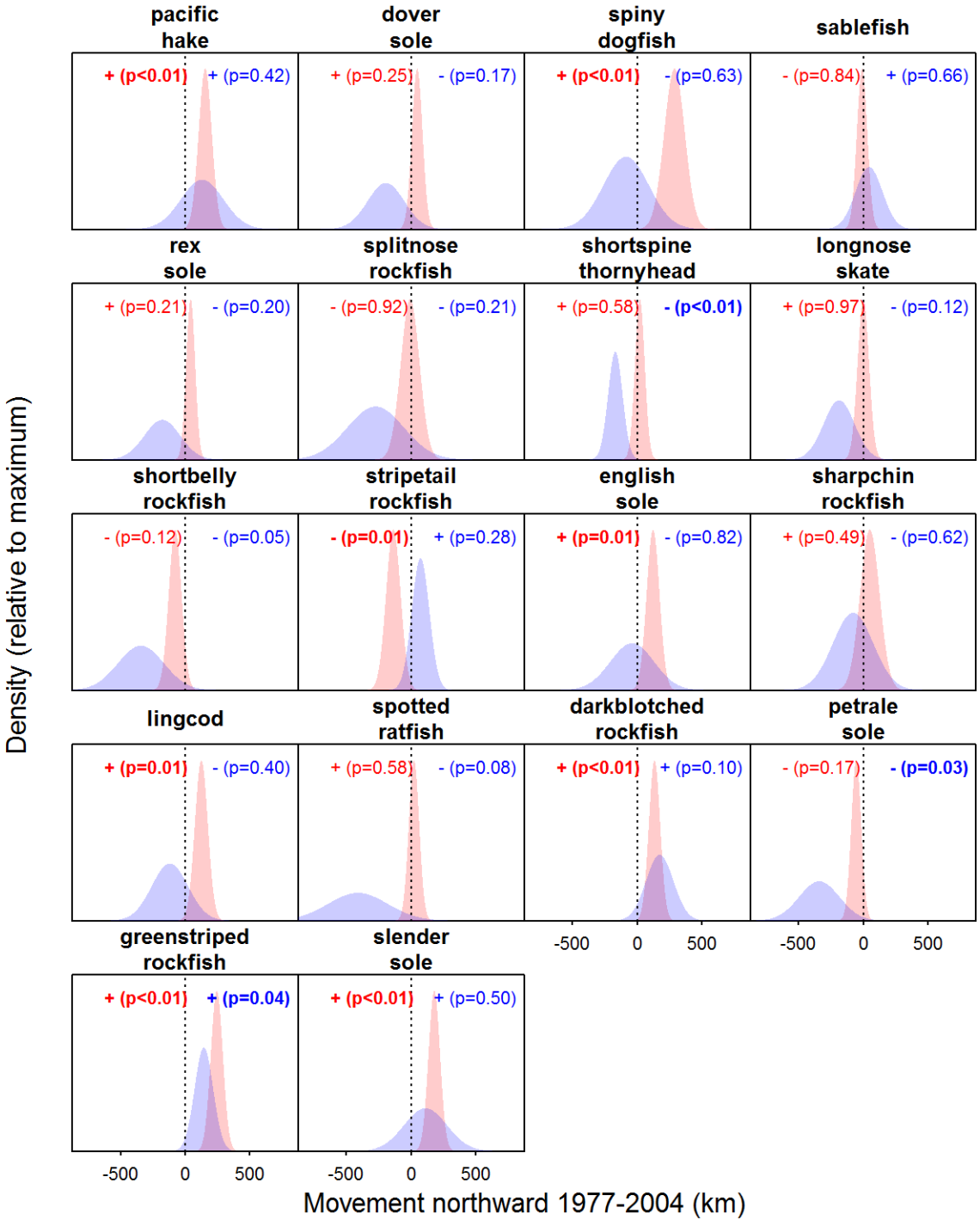
pacific hake
+ (p<0.01)
+ (p=0.42)
dover sole
+ (p=0.25)
- (p=0.17)
spiny dogfish
+ (p<0.01)
- (p=0.63)
sablefish
- (p=0.84)
+ (p=0.66)
rex sole
+ (p=0.21)
- (p=0.20)
splitnose rockfish
- (p=0.92)
- (p=0.21)
shortspine thornyhead
+ (p=0.58)
- (p<0.01)
longnose skate
+ (p=0.97)
- (p=0.12)
shortbelly rockfish
- (p=0.12)
- (p=0.05)
stripetail rockfish
- (p=0.01)
+ (p=0.28)
english sole
+ (p=0.01)
- (p=0.82)
sharpchin rockfish
+ (p=0.49)
- (p=0.62)
lingcod
+ (p=0.01)
- (p=0.40)
spotted ratfish
+ (p=0.58)
- (p=0.08)
darkblotched rockfish
+ (p<0.01)
+ (p=0.10)
petrale sole
- (p=0.17)
- (p=0.03)
greenstriped rockfish
+ (p<0.01)
+ (p=0.04)
slender sole
+ (p<0.01)
+ (p=0.50)
-500
0
500
Density (relative to maximum)
Movement northward 1977-2004 (km)

672

673 **Fig. 7**

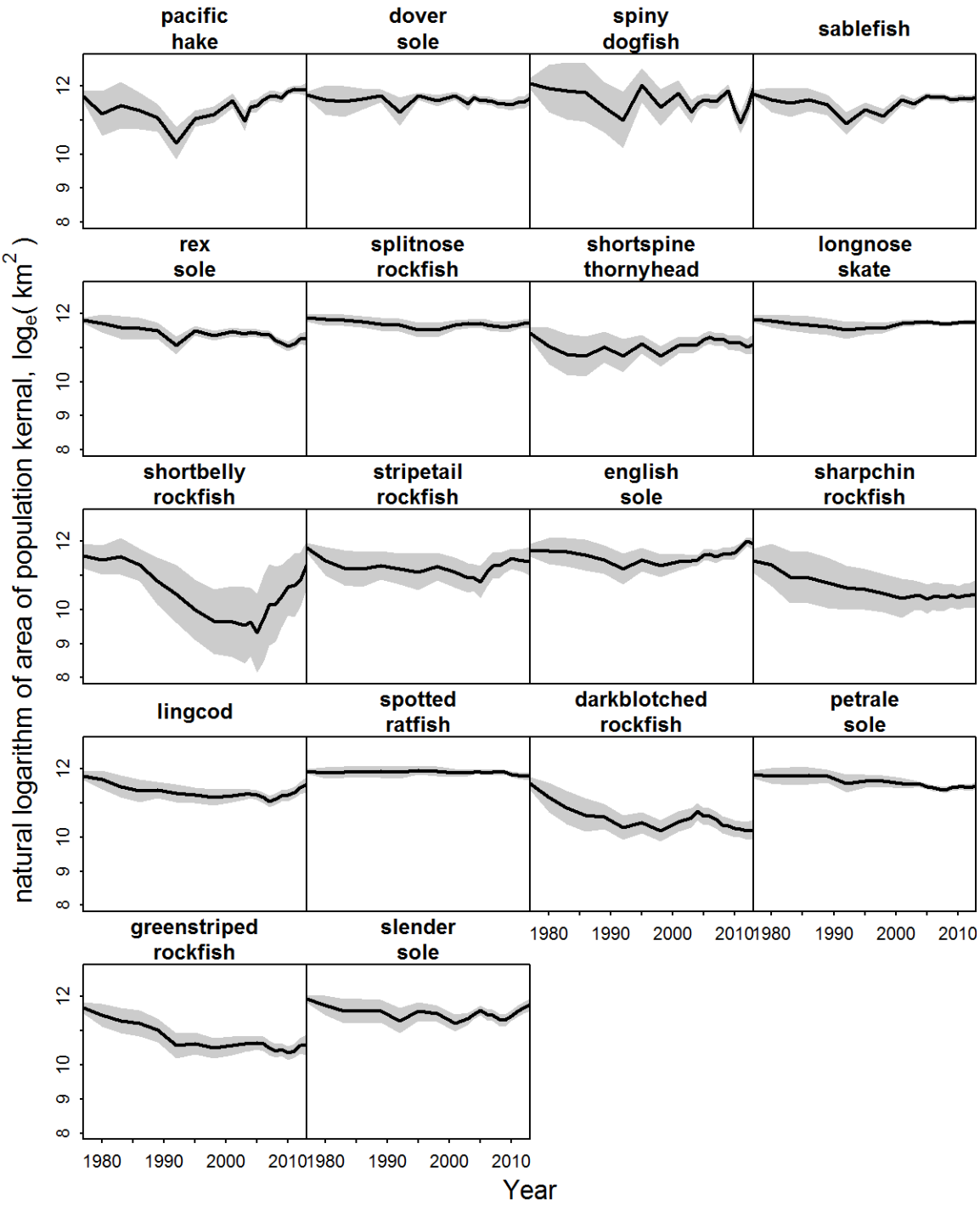
pacific hake
dover sole
spiny dogfish
sablefish
rex sole
splitnose rockfish
shortspine thornyhead
longnose skate
shortbelly rockfish
stripetail rockfish
english sole
sharpchin rockfish
lingcod
spotted ratfish
darkblotched rockfish
petrale sole
greenstriped rockfish
slender sole
natural logarithm of area of population kernal, log$_e$(km^2)
8
9
10
12
1980
1990
2000
2010
Year

674

675 **Fig. 8**

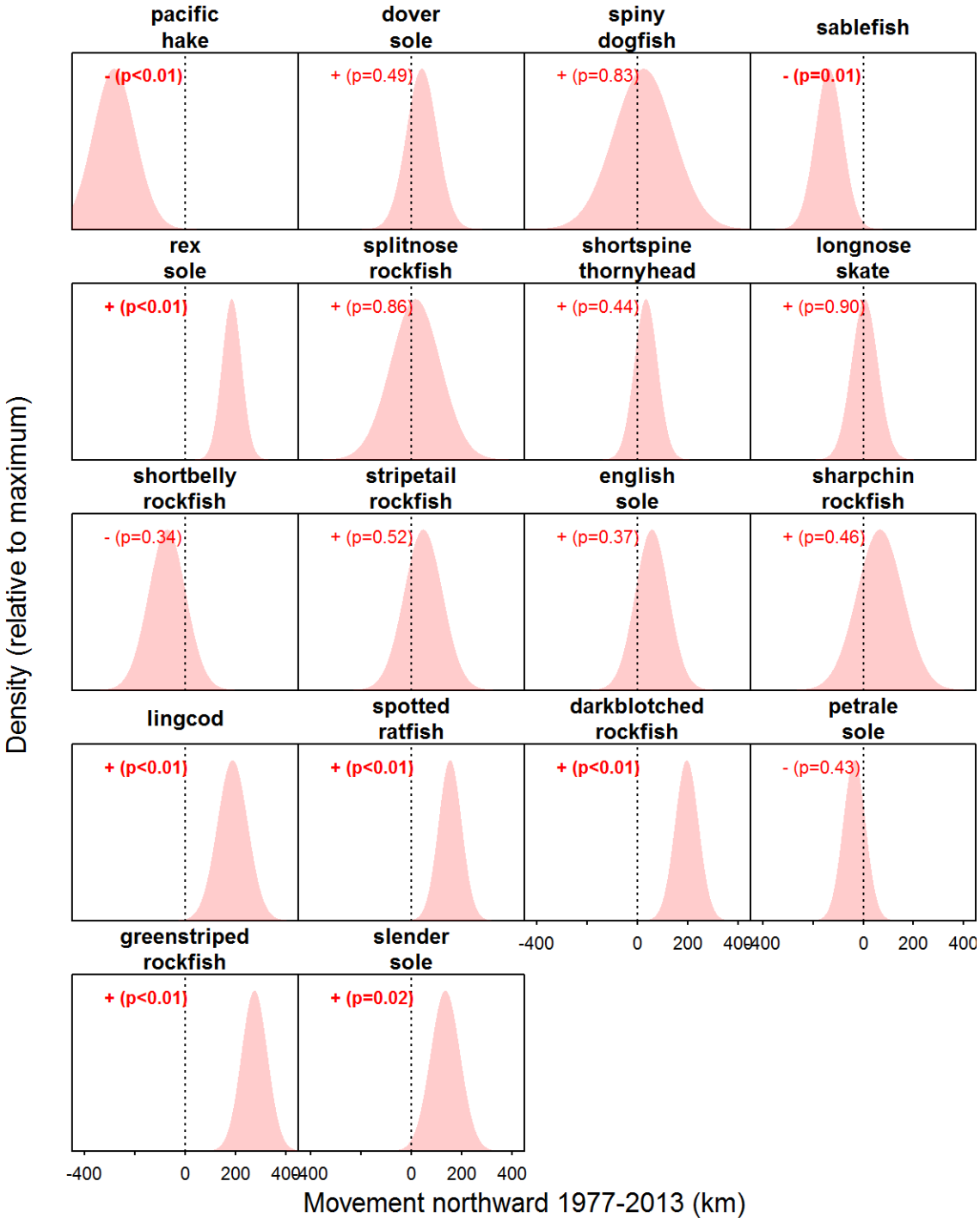
pacific hake
- (p<0.01)
dover sole
+ (p=0.49)
spiny dogfish
+ (p=0.83)
sablefish
- (p=0.01)
rex sole
+ (p<0.01)
splitnose rockfish
+ (p=0.86)
shortspine thornyhead
+ (p=0.44)
longnose skate
+ (p=0.90)
shortbelly rockfish
- (p=0.34)
stripetail rockfish
+ (p=0.52)
english sole
+ (p=0.37)
sharpchin rockfish
+ (p=0.46)
lingcod
+ (p<0.01)
spotted ratfish
+ (p<0.01)
darkblotched rockfish
+ (p<0.01)
petrale sole
- (p=0.43)
greenstriped rockfish
+ (p<0.01)
slender sole
+ (p=0.02)
-400
0
200
400
Density (relative to maximum)
Movement northward 1977-2013 (km)

676